

Dinuclear Copper(II) Complexes of the Tetradentate Thiadiazole Ligands BPMTD (2,5-Bis((2-pyridylmethyl)thio)thiadiazole) and BPTD (2,5-Bis(2-pyridylthio)thiadiazole). X-ray Structures of $[\text{Cu}_2(\text{BPTD})(\mu_2\text{-Br})_2\text{Br}_2]$ and $[\text{Cu}(\text{BPMTD})\text{Cl}_2]_n$ and Spectroscopic, Electrochemical, and Magnetic Studies

Santokh S. Tandon, Liqin Chen, Laurence K. Thompson,* and John N. Bridson

Department of Chemistry, Memorial University of Newfoundland,
St. John's, Newfoundland, Canada A1B 3X7

Received August 6, 1993*

Dinuclear copper(II) complexes of two new, tetradentate (N_4), dinucleating ligands 2,5-bis((2-pyridylmethyl)thio)thiadiazole (BPMTD) and 2,5-bis(2-pyridylthio)thiadiazole (BPTD) are described. The complexes $[\text{Cu}_2(\text{BPMTD})(\mu_2\text{-Cl})_2\text{Cl}_2] \cdot 2\text{CH}_3\text{OH} \cdot 0.5\text{CH}_3\text{CN}$ (**1**), $[\text{Cu}_2(\text{BPTD})(\mu_2\text{-X})_2\text{X}_2]$ ($\text{X} = \text{Cl}$ (**2**), $\text{X} = \text{Br}$ (**3**)), $[\text{Cu}_2(\text{BPTD})(\mu_2\text{-OH})(\text{NO}_3)_3]$ (**4**), and $[\text{Cu}(\text{BPMTD})\text{Cl}_2]_n$ (**5**) were isolated and the X-ray crystal structures of **3** and **5** determined. **3** crystallized in the monoclinic system, space group $C2/c$, with $a = 11.750(2)$ Å, $b = 14.235(3)$ Å, $c = 12.243(3)$ Å, $\beta = 107.53(2)^\circ$, and $Z = 4$ ($R = 0.031$ and $R_w = 0.027$). **5** crystallized in the orthorhombic system, space group $Pbca$, with $a = 15.088(4)$ Å, $b = 13.642(8)$ Å, $c = 8.986(4)$ Å, and $Z = 4$ ($R = 0.058$ and $R_w = 0.054$). In **3** two slightly distorted square-pyramidal copper(II) centers are bridged simultaneously by the diazole (N_2) and by two halogens in an axial-equatorial arrangement. A preliminary structure for **1** indicates a similarly bridged species, but Cu–Cu separations differ markedly (3.224(4) Å (**1**); 3.556(2) Å (**3**)), due to the different chelate ring sizes. Low room-temperature magnetic moments and variable-temperature magnetic studies (4–300 K) indicate the presence of weak antiferromagnetic exchange in **1–3** and strong antiferromagnetic exchange in **4**. For the first time, the thiadiazole N_2 group is examined as a superexchange bridge between copper(II) centers and is found to propagate spin coupling less effectively than pyridazine or phthalazine (thiadiazole < phthalazine < pyridazine). Cyclic voltammograms for **1–3** in DMF are typical for one-step, two-electron, quasi-reversible redox processes associated with the $\text{Cu}^{\text{II}}/\text{Cu}^{\text{I}}$ redox couple. A most unusual 1-dimensional, zigzag, polymeric dinuclear structure exists in **5**, with no involvement of the thiadiazole nitrogens in bonding to copper, but with the peripheral pyridine rings linking the six-coordinate copper(II) centers, which involve an equatorial CuN_2Cl_2 donor set and long axial interactions with exocyclic sulfur atoms.

Introduction

In continuing our interest in the magneto-structural properties of dinuclear and polynuclear metal complexes of polydentate, noncyclic $\mu_{1,2}$ -diazine ligands,^{1–14} we have isolated two new, potentially tetradentate, dinucleating thiadiazole ligands, 2,5-bis((2-pyridylmethyl)thio)thiadiazole (BPMTD) and 2,5-bis(2-pyridylthio)thiadiazole (BPTD), which on coordination with metal centers would be expected to form two adjacent seven-membered

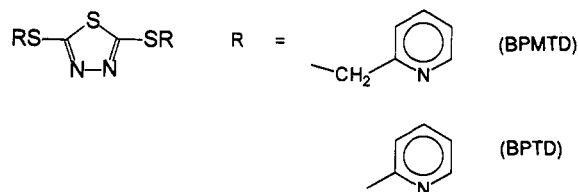


Figure 1. of the ligands BPMTD and BPTD.

- * Author to whom correspondence should be addressed.
 © Abstract published in *Advance ACS Abstracts*, December 15, 1993.
 (1) Thompson, L. K.; Lee, F. L.; Gabe, E. J. *Inorg. Chem.* **1988**, *27*, 39 and references therein.
 (2) Chen, L.; Thompson, L. K.; Bridson, J. N. *Inorg. Chem.* **1993**, *32*, 2938.
 (3) Tandon, S. S.; Mandal, S. K.; Thompson, L. K.; Hynes, R. C. *Inorg. Chem.* **1992**, *31*, 2215.
 (4) Tandon, S. S.; Mandal, S. K.; Thompson, L. K.; Hynes, R. C. *J. Chem. Soc., Chem. Commun.* **1992**, 1572.
 (5) Tandon, S. S.; Thompson, L. K.; Hynes, R. C. *Inorg. Chem.* **1992**, *31*, 2210.
 (6) Chen, L.; Thompson, L. K.; Bridson, J. N. *Inorg. Chim. Acta* **1993**, *214*, 67.
 (7) Tandon, S. S.; Thompson, L. K.; Bridson, J. N. *J. Chem. Soc., Chem. Commun.* **1993**, 804.
 (8) Thompson, L. K.; Mandal, S. K.; Charland, J.-P.; Gabe, E. J. *Can. J. Chem.* **1988**, *66*, 348.
 (9) Mandal, S. K.; Thompson, L. K.; Gabe, E. J.; Charland, J.-P.; Lee, F. L. *Inorg. Chem.* **1988**, *27*, 855.
 (10) Mandal, S. K.; Thompson, L. K.; Newlands, M. J.; Charland, J.-P.; Gabe, E. J. *Inorg. Chim. Acta* **1990**, *178*, 169.
 (11) Lacroix, P.; Kahn, O.; Valade, L.; Cassoux, P.; Thompson, L. K. *Synth. Met.* **1990**, *39*, 81.
 (12) Tandon, S. S.; Chen, L.; Thompson, L. K.; Connors, S. P.; Bridson, J. N. *Inorg. Chim. Acta* **1993**, *213*, 289.
 (13) Tandon, S. S.; Thompson, L. K.; Bridson, J. N. *Inorg. Chem.* **1993**, *32*, 32.
 (14) Wen, T.; Thompson, L. K.; Lee, F. L.; Gabe, E. J. *Inorg. Chem.* **1988**, *27*, 4190.

and six-membered chelate rings, respectively, in a dinuclear structural arrangement. One objective of the present study is to investigate the exchange interactions between copper(II) centers via the thiadiazole bridge and to study the effect of the chelate ring size on the structural and magnetic properties. Although 1,3,4-thiadiazole is itself a potentially versatile ligand, very little has been reported on this system or its derivatives.^{15–18}

In a recent communication,⁷ we reported the X-ray crystal structure and magnetic properties of a dinuclear, ferromagnetically coupled μ_2 -1,1-azide-bridged copper(II) complex, $[\text{Cu}_2(\text{BPMTD})(\mu_2\text{-Br})(\mu_2\text{-1,1-N}_3)\text{Br}_2] \cdot \text{CH}_3\text{CN}$. Here we report the synthetic, spectroscopic, and electrochemical properties and variable-temperature magnetic studies of a series of dinuclear copper(II) complexes of the structurally related ligands BPMTD and BPTD (Figure 1), which exhibit weak to strong ($-2J = 34-$

- (15) Fabretti, A. C.; Malavasi, W.; Gatteschi, D.; Sessoli, R. *Inorg. Chim. Acta* **1992**, *195*, 157.
 (16) Antolini, L.; Benedetti, A.; Fabretti, A. C.; Giusti, A.; Menziani, M. C. *J. Chem. Soc., Dalton Trans.* **1988**, 1075.
 (17) Antolini, L.; Benedetti, A.; Fabretti, A. C.; Giusti, A. *J. Chem. Soc., Dalton Trans.* **1988**, 2501.
 (18) Ferrer, S.; Borrás, J.; Miratvilles, C.; Fuentes, A. *Inorg. Chem.* **1990**, *29*, 206.

530 cm⁻¹) antiferromagnetic exchange interactions between adjacent copper centers. X-ray crystal structures of the dinuclear complexes **1** (preliminary) and **3** have been determined and are shown to involve conventional dinuclear centers with $\mu_{1,2}$ -thiadiazole-*N,N'*-bridges. In addition a 1-dimensional, polymeric chain complex, **5**, is also reported, which, although dinuclear, does not involve thiadiazole bonding.

Experimental Section

Synthesis of the Ligands. (a) **2,5-Bis((2-pyridylmethyl)thio)thiadiazole (BPMTD).** Sodium metal (3.70 g, 160 mmol) was dissolved in 200 mL of dry (O₂ free) methanol by stirring at room temperature for 30 min (N₂ atmosphere). 2,5-Dimercapto-1,3,4-thiadiazole (6.00 g, 40 mmol) was added, and the resulting light brown solution was stirred at -5 to 0 °C for 1 h. 2-Picolyl chloride hydrochloride (13.1 g, 80 mmol) dissolved in 100 mL of dry methanol (O₂ free) was added, dropwise over a period of 1.5 h, keeping the temperature at ca. 0 °C. After the complete addition, the resulting mixture was stirred at 0 °C for 1 h, then at 60–70 °C for 4 h, and finally at room temperature for 16 h. A white solid (NaCl) precipitated, which was filtered off, and the filtrate was concentrated under reduced pressure at 30 °C to give an oily mass, which solidified on cooling to produce a white crystalline compound. It was characterized through mass and NMR spectra. Yield: 9.0 g (68%). Mp: 82–83 °C. Mass spectrum (*m/e*): 332 (P). ¹H NMR (CDCl₃) (δ , ppm (relative intensity)): 5.79 (singlet, 4H, CH₂), 7.22 (triplet, 2H, Py), 7.46 (doublet, 2H, Py), 7.65 (triplet, 2H, Py), 8.57 (doublet, 2H, Py).

In an initial reaction to produce BPMTD, carried out in refluxing, undried ethanol (no exclusion of air), a brown oil was obtained, after chloroform extraction, which did not solidify on standing. The oil was purified by chromatography (silica gel) using CHCl₃ as eluent. In an attempt to characterize this species, a portion was reacted with an excess of Cu(NO₃)₂·3H₂O in acetonitrile/methanol (4:1). A deep blue solution formed on standing at room temperature for several days, producing blue crystals in high yield, which were characterized by X-ray diffraction studies and shown to be [Cu(BPMS)(NO₃)₂] (BPMS = bis(2-pyridylmethyl) sulfide).¹⁹ No other product was identified in the reaction mixture. BPMS is considered to have resulted during ligand synthesis by base-induced nucleophilic attack on BPMTD, or its half-substituted precursor, at the C₁ position, to produce the 2-pyridylmethanethiolate anion, which then reacts with 2-(chloromethyl)pyridine. No evidence exists for the ultimate formation of BPMTD in this reaction, and subsequent preparations (see above) used dried methanol in the absence of air for the successful synthesis of BPMTD. The fact remains, however, that BPMTD or its monosubstituted precursor is unstable.

(b) **2,5-Bis((2-pyridylthio)thiadiazole (BPTD).** BPTD was prepared by the same method used for the synthesis of BPMTD, by replacing 2-(chloromethyl)pyridine with 2-bromopyridine. Mp: 86–88 °C. Yield 42%. Mass spectrum (*m/e*): 304 (P). ¹H NMR (CDCl₃) (δ , ppm (relative intensity)): 7.25 (triplet, 2H, Py), 7.43 (doublet, 2H, Py), 7.67 (triplet, 2H, Py), 8.55 (doublet, 2H, Py).

Synthesis of the Complexes. [Cu₂(BPMTD)(μ_2 -Cl₂)Cl₂·2CH₃OH·0.5CH₃CN (**1**), [Cu₂(BPTD)(μ_2 -X₂)₂X₂] (X = Cl (**2**), X = Br (**3**)), and [Cu₂(BPTD)(μ_2 -OH)(NO₃)₃] (**4**). 2,5-Bis((2-pyridylmethylthio)thiadiazole (BPMTD) (0.20 g, 0.60 mmol), dissolved in a mixture of acetonitrile/methanol (1:1; 40 mL), was added to a solution of copper(II) chloride (0.17 g, 1.0 mmol) in 20 mL of methanol. On standing overnight, the resulting green solution produced bright green crystals, suitable for X-ray diffraction studies, which were filtered off, washed with a mixture of methanol/acetonitrile (1:1) (3 × 5 mL), and dried under vacuum. Yield: 75% (**1**). Anal. Calcd for [Cu₂(C₁₄H₁₂N₄S₃)(μ_2 -Cl₂)Cl₂·2CH₃OH·0.5CH₃CN (**1**): C, 29.77; H, 3.15; N, 9.21; Cu, 18.53. Found: C, 29.20; H, 2.76; N, 9.44; Cu, 18.00. Compound **2** was prepared similarly, as a green crystalline solid, by reacting BPTD with CuCl₂·2H₂O in a mixture of methanol/chloroform (1:1). Yield: 60%. Anal. Calcd for [Cu₂(C₁₂H₈N₄S₃)(μ_2 -Cl₂)Cl₂] (**2**): C, 25.14; H, 1.41; N, 9.77. Found: C, 24.82; H, 1.45; N, 9.92. **3** was obtained in a similar manner, as dark brown crystals suitable for X-ray diffraction studies, by reacting BPTD with CuBr₂. Yield: 69%. Anal. Calcd for [Cu₂(C₁₂H₈N₄S₃)(μ_2 -Br)₂-Br₂] (**3**): C, 19.19; H, 1.07; N, 7.46. Found: C, 19.91; H, 1.17; N, 7.94. **4** was prepared similarly, as a blue microcrystalline solid. Yield: 63%. Anal. Calcd for [Cu₂(C₁₂H₈N₄S₃)(μ_2 -OH)(NO₃)₃] (**4**): C, 22.71; H, 1.43; N, 15.43. Found: C, 22.90; H, 1.53; N, 15.72.

[Cu(BPMTD)Cl₂]_n (**5**). A solution of Cu(ClO₄)₂·6H₂O (0.500 g, 1.35 mmol) dissolved in MeOH (20 mL) was added to a solution of BPMTD (0.15 g, 0.45 mmol) in a mixture of MeOH/CH₃CN (20/10 mL). The resulting green solution was stirred at room temperature for 10 min. A solution of NH₄Cl (0.3 g) dissolved in MeOH (20 mL) was added, giving a bright green solution. Green crystals suitable for X-ray analysis appeared after a few hours and were filtered off, washed with MeO, and dried. Yield: 0.18 g, 85%.

Physical Measurements. NMR spectra were recorded with a Bruker WP80 spectrometer (SiMe₄ internal standard), and mass spectra were obtained with a VG Micromass 7070 HS spectrometer with a direct-insertion probe. Electronic spectra were recorded as mulls and in DMF solutions using a Cary 5E spectrometer. Infrared spectra were recorded as Nujol mulls using a Mattson Polaris FT-IR instrument. ESR spectra were obtained using a Bruker ESP 300 X-band spectrometer at room temperature and 77 K. Room-temperature magnetic moments were measured by the Faraday method using a Cahn 7600 Faraday magnetic balance, and variable-temperature magnetic data (4–300 K) were obtained using an Oxford Instruments superconducting Faraday susceptometer with a Sartorius 4432 microbalance. A main solenoid field of 1.5 T and a gradient field of 10 T m⁻¹ were employed.

Electrochemical measurements were performed at room temperature in dimethylformamide (DMF) (spectroquality grade dried over molecular sieves) under O₂-free conditions using a BAS CV-27 voltammograph and a Hewlett-Packard 7005B X-Y recorder. For cyclic voltammetry, a three-electrode system was used, with a glassy carbon working electrode, platinum counter electrode, and a saturated calomel (SCE) reference electrode. For constant-potential electrolysis (CPE) a three-component "H" cell was used, with a central 5-mL working compartment separated from auxiliary and reference compartments by medium-porosity sintered-glass frits. The working electrode was a platinum mesh "flag", the auxiliary electrode a platinum wire, and the reference electrode was a silver wire. The supporting electrolyte was 0.1M tetraethylammonium perchlorate (TEAP). All potentials are reported versus the saturated calomel electrode (SCE). For cyclic voltammetry, all solutions were 10⁻³–10⁻⁴ M in complex. Microanalyses were carried out by the Canadian Microanalytical Service, Delta, Canada, and copper was determined by EDTA titrations.

Crystallographic Data Collection and Refinement for the Structures. [Cu₂(BPTD)(μ_2 -Br)₂Br₂] (**3**) and [Cu(BPMTD)Cl]_n (**5**). The crystals of **3** are dark brown, almost black in appearance. The diffraction intensities of an approximately 0.3 × 0.3 × 0.2 mm regular polyhedral crystal were collected with graphite-monochromatized Mo K α radiation using a Rigaku AFC6S diffractometer at 26 ± 1 °C using the ω -2 θ scan technique to a 2 θ_{max} value of 50.0°. A total of 1876 reflections were measured, of which 1783 (*R*_{int} = 0.040) were unique and 1319 were considered significant with *I*_{net} > 2.00 σ (*I*_{net}). An empirical absorption correction was applied, after a full isotropic refinement, using the program DIFABS,²⁰ which resulted in transmission factors ranging from 0.39 to 1.00. The data were corrected for Lorentz and polarization effects. The cell parameters were obtained from the least-squares refinement of the setting angles of 20 carefully centered reflections with 2 θ in the range 41.67–46.95°.

The structure was solved by direct methods.^{21,22} The non-hydrogen atoms were refined anisotropically. The final cycle of full-matrix least-squares refinement was based on 1319 observed reflections (*I* > 2.00 σ (*I*)) and 115 variable parameters and converged with unweighted and weighted agreement factors of *R* = $\sum(|F_o| - |F_c|) / \sum|F_o| = 0.036$ and *R*_w = $[(\sum w(|F_o| - |F_c|)^2) / \sum w F_o^2]^{1/2} = 0.032$. The maximum and minimum peaks on the final difference Fourier map correspond to 0.62 and -0.56 electron/Å³, respectively. Neutral-atom scattering factors²³ and anomalous-dispersion terms^{24,25} were taken from the usual sources. All calculations were performed with the TEXSAN²⁶ crystallographic software package using a VAX 3100 work station. A summary of the crystal and other data is given in Table 1, and atomic coordinates are given in Table 2. Hydrogen atom coordinates (Table S1), anisotropic

(20) Walker, N.; Stuart, D. *Acta Crystallogr., Sect. A* 1983, 39, 158.

(21) Gilmore, C. J. *J. Appl. Crystallogr.* 1984, 17, 42.

(22) Beurskens, P. T. DIRDIF. Technical Report 1984/1; Crystallography Laboratory: Toernooiveld, 6525 Ed Nijmegen, The Netherlands.

(23) Cromer, D. T.; Waber, J. T. *International Tables for X-ray Crystallography*; Kynoch Press: Birmingham, U.K., 1974; Vol. IV, Table 2.2A.

(24) Ibers, J. A.; Hamilton, W. C. *Acta Crystallogr.* 1974, 17, 781.

(25) Cromer, D. T. *International Tables for X-ray Crystallography*; Kynoch Press: Birmingham, U.K., 1974; Vol. IV, Table 2.3.1.

(26) *Texsan-Textray Structure Analysis Package*. Molecular Structure Corp.: The Woodlands, TX, 1985.

(19) Tandon, S. S.; Thompson, L. K.; Bridson, J. N. Unpublished results.

Table 1. Summary of Crystallographic Data for [Cu₂(BPTD)(μ₂-Br)₂Br₂] (3) and [Cu(BPMTD)Cl₂]_n (5)

	3	5
empirical formula	C ₁₂ H ₈ N ₄ S ₃ Br ₄ Cu ₂	C ₁₄ H ₁₂ N ₄ S ₃ Cl ₂ Cu
fw	751.11	466.91
space group	C2/c (No. 15)	Pbca (No. 61)
a (Å)	11.750(2)	15.088(4)
b (Å)	14.235(3)	13.642(8)
c (Å)	12.243(3)	8.986(4)
β (deg)	107.53(2)	
V (Å ³)	1952.6(7)	1850(2)
ρ _{calcd} (g cm ⁻³)	2.555	1.677
Z	4	4
μ (cm ⁻¹)	106.10	18.04
λ (Å)	0.710 69	0.710 69
T (°C)	26	26
R ^a	0.031	0.058
R _w ^b	0.027	0.054

$$^a R = \sum(|F_o| - |F_c|) / \sum|F_o|. \quad ^b R_w = [\sum w(|F_o| - |F_c|)^2 / \sum w F_o^2]^{1/2}.$$

Table 2. Final Atomic Positional Parameters and B(eq) Values (Å²) for [Cu₂(BPTD)(μ₂-Br)₂Br₂] (3)

atom	x	y	z	B(eq) ^a
Br(1)	0.17569(7)	0.44050(5)	0.07571(6)	3.47(3)
Br(2)	0.48227(6)	0.41929(4)	0.10393(6)	3.02(3)
Cu(1)	0.34181(7)	0.35550(5)	0.19289(7)	2.29(3)
S(1)	0.2398(1)	0.1321(1)	0.1771(2)	3.04(7)
S(2)	1/2	0.0632(2)	1/4	3.3(1)
N(1)	0.2391(4)	0.2996(3)	0.2837(4)	2.2(2)
N(2)	0.4397(4)	0.2347(3)	0.2309(4)	2.1(2)
C(1)	0.2013(6)	0.3574(4)	0.3541(6)	2.8(3)
C(2)	0.1256(6)	0.3282(5)	0.4144(6)	3.1(3)
C(3)	0.0923(6)	0.2357(5)	0.4074(6)	3.6(3)
C(4)	0.1315(6)	0.1742(4)	0.3406(6)	3.0(3)
C(5)	0.2031(5)	0.2084(4)	0.2766(5)	2.3(3)
C(6)	0.3936(5)	0.1506(4)	0.2192(5)	2.4(3)

$$^a B(\text{eq}) = (8\pi^2/3) \sum_{i=1}^3 \sum_{j=1}^3 U_{ij} a_i^* a_j^* \bar{a}_i \bar{a}_j.$$

thermal parameters (Table S2), a full listing of bond distances and angles (Table S3), and least-squares-planes data (Table S4) are included as supplementary material.

[Cu(BPMTD)Cl₂]_n (5). The X-ray sample comprised crystals showing distinct zoning effects under the microscope, which suggested the possibility of twinning. However indexing proceeded normally and the Laue symmetry check was successful. Diffraction data collection and structural refinement for 5 were carried out in a manner similar to that for 3. Hydrogen atoms were placed in calculated positions, with isotropic thermal parameters 20% greater than those of their bonded partners. They were included, but not refined, in the last round of least-squares refinement. The data set was rather weak and did not justify a fully anisotropic refinement. Consequently, the carbon atoms were refined isotropically and all other non-hydrogen atoms refined anisotropically. The solution shows a linear polymeric structure and may be interpreted as the disordered superposition of two opposite "zigzag" chains, each with 50% occupancy. Alternatively, the crystal may have a continuous lattice, but the macroscopic zoning, which divides the crystal into four regions of approximately equal volumes, could indicate a discontinuity in the polymeric structure. This possibility is under further investigation. Pertinent crystallographic and other data are given in Table 1, and atomic coordinates are given in Table 3. Hydrogen atom coordinates (Table S5), thermal parameters (Tables S6), and a complete listing of bond distances and angles (Tables S7) are included as supplementary material.

A structural determination was carried out on 1, but gave a poor refinement ($R = 0.126$, $R_w = 0.124$; space group $P2_1/c$, $a = 7.460(3)$ Å, $b = 22.428(3)$ Å, $c = 15.433(2)$ Å, $\beta = 98.82(2)^\circ$, $V = 2552(1)$ Å³). However the main structural fragment is clearly defined (Figure 2).

Results and Discussion

Synthesis of BPMTD Complexes. The successful synthesis of dinuclear copper(II) complexes of BPMTD appears to be dependent on the nature of the anion used. Tetradentate diazine ligands like BPMTD would provide only two nitrogen donor centers per metal (diazine and peripheral pyridine nitrogens) in a conventional dinuclear structural arrangement, and in the

Table 3. Final Atomic Positional Parameters and B(eq) Values (Å²) for [Cu(BPMTD)Cl]_n (5)

atom	x	y	z	B(eq) ^a
Cu(1)	0	0	0	3.47(7)
Cl(1)	-0.0686(2)	0.1191(2)	-0.1366(3)	5.0(1)
S(1)	0.0334(4)	-0.1188(5)	-0.2472(7)	4.4(3)
S(2)	0.0157(4)	0.0262(4)	-0.502(1)	4.8(4)
S(3)	-0.0908(5)	0.0887(5)	0.2350(7)	4.4(3)
N(1)	-0.1130(4)	-0.0817(6)	-0.005(1)	3.9(4)
N(2)	-0.098(1)	-0.108(1)	-0.448(2)	5(1)
N(3)	-0.129(1)	-0.059(1)	0.423(2)	5(1)
C(1)	-0.1838(7)	-0.0534(9)	0.074(1)	5.0(3)
C(2)	-0.2621(8)	-0.110(1)	0.077(1)	6.5(3)
C(3)	-0.2638(8)	-0.192(1)	-0.005(1)	7.6(3)
C(4)	-0.1943(8)	-0.223(1)	-0.088(1)	7.2(3)
C(5)	-0.1191(8)	-0.1651(9)	-0.082(1)	5.5(3)
C(6)	-0.046(1)	-0.206(2)	-0.168(2)	5.4(5)
C(7)	-0.025(1)	-0.073(1)	-0.398(2)	3.2(4)
C(8)	-0.075(1)	0.012(1)	0.387(2)	3.7(4)
C(9)	-0.194(1)	0.036(2)	0.157(2)	4.7(5)

$$^a B(\text{eq}) = (8\pi^2/3) \sum_{i=1}^3 \sum_{j=1}^3 U_{ij} a_i^* a_j^* \bar{a}_i \bar{a}_j.$$

absence of other suitable ligand groups, the formation of a dinuclear species may be inhibited. However, because the exocyclic sulfur atoms could take part in the formation of five-membered chelate rings with the pyridine nitrogen atoms, NS coordination by BPMTD is also a possibility (vide infra). Also, complex formation is complicated by redox processes associated with the ligand and the anion. With CuCl₂ in a CH₃CN/MeOH mixture, a dinuclear, five-coordinate copper(II) complex (1) is produced after allowing the reaction mixture to stand overnight. However, with copper bromide, although dinuclear species appear to be formed under similar conditions, analytical data indicate that some decomposition has occurred with the formation of mixed-oxidation-state (Cu^{II}/Cu^I) species. This is confirmed by the observation of a very strong axial ESR signal (solid at room temperature; $g_{\perp} = 2.06$, $g_{\parallel} = 2.15$) typical of a dilute copper(II) center. However, a well-defined copper(II) bromide complex could not be successfully characterized. With CuX₂ (X = NO₃, ClO₄) in a CH₃CN/MeOH mixture, dinuclear complexes could not be isolated, and in fact, a spontaneous redox reaction occurs on allowing the reaction mixture to stand for several days, producing colorless [Cu(CH₃CN)₄]X as the major product, thus indicating probable ligand decomposition by a hydrolytic process and the formation of an intermediate thiol, which is then responsible for reduction of copper(II). That this does not appear to happen to a significant extent with copper chloride indicates the importance of this anion as a ligand in the stabilization of the dinuclear copper(II) complex, a role which perchlorate and nitrate perform much less effectively. With copper bromide, however, a redox reaction does occur, with incomplete reduction to copper(I), which may also be associated with the presence of bromide itself.

Complex 5 was prepared as a stable complex in high yield by the immediate addition of chloride to a solution of copper perchlorate and BPMTD in CH₃CN/MeOH. This suggests that, at least initially, a copper(II) perchlorate complex of BPMTD exists in solution.

Description of the Structures of [Cu₂(BPMTD)(μ₂-Cl)₂Cl₂·H₂O (1), [Cu₂(BPTP)(μ₂-Br)₂Br₂] (3), and [Cu(BPMTD)Cl]_n (5). The structure of 1 is shown in the Figure 2. Two somewhat distorted square-pyramidal copper centers are bound to the tetradentate thiazazole ligand (BPMTD), with the formation of seven-membered chelate rings, and bridged by the thiazazole nitrogen atoms (N(2), N(3)) and two chlorine atoms (Cl(1), Cl(2)) in a triple-bridged arrangement. The chlorine bridges are involved in equatorial and axial interactions with each copper center, with Cu(1)-Cl(1)-Cu(2) and Cu(1)-Cl(2)-Cu(2) bridge angles of 84.1(3)° and 84.0(2)°, respectively, which are comparable to those reported for similar triply bridged dicopper(II) complexes

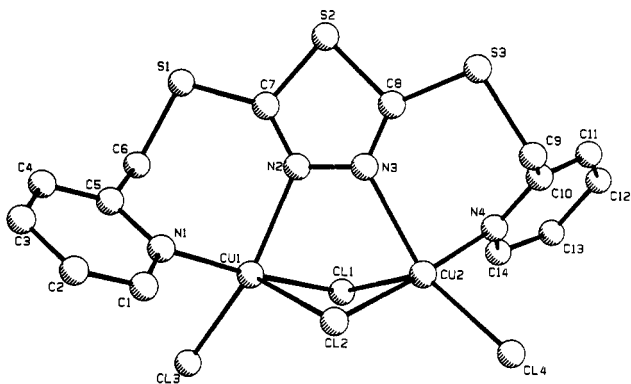


Figure 2. representation of $[\text{Cu}_2(\text{BPMTD})\text{Cl}_4]$ (1). Bond distances (Å) and angles (deg): $\text{Cu}(1)\text{--Cu}(2) = 3.224(4)$, $\text{Cu}(1)\text{--N}(1) = 2.02(2)$, $\text{Cu}(1)\text{--N}(2) = 2.21(2)$, $\text{Cu}(1)\text{--Cl}(1) = 2.310(8)$, $\text{Cu}(1)\text{--Cl}(2) = 2.533(8)$, $\text{Cu}(1)\text{--Cl}(3) = 2.245(8)$, $\text{Cu}(2)\text{--N}(3) = 2.27(2)$, $\text{Cu}(2)\text{--Cl}(1) = 2.501(8)$, $\text{Cu}(2)\text{--Cl}(2) = 2.276(8)$, $\text{Cu}(2)\text{--N}(4) = 1.99(2)$, $\text{Cu}(2)\text{--Cl}(4) = 2.236(7)$; $\text{Cu}(1)\text{--Cl}(1)\text{--Cu}(2) = 84.1(3)$, $\text{Cu}(1)\text{--Cl}(2)\text{--Cu}(2) = 84.0(2)$, $\text{Cu}(1)\text{--N}(2)\text{--N}(3) = 112(1)$, $\text{Cu}(2)\text{--N}(3)\text{--N}(2) = 116(1)$, $\text{Cl}(3)\text{--Cu}(1)\text{--N}(2) = 158.8(6)$, $\text{N}(1)\text{--Cu}(1)\text{--Cl}(1) = 173.1(6)$, $\text{N}(4)\text{--Cu}(2)\text{--Cl}(2) = 174.9(7)$, $\text{N}(3)\text{--Cu}(2)\text{--Cl}(4) = 150.0(6)$.

involving related tetradentate (N_4) diazine ligands.²⁷ The equatorial copper–chlorine bridge bond lengths ($\text{Cu}(1)\text{--Cl}(1) = 2.310(8)$ Å, $\text{Cu}(2)\text{--Cl}(2) = 2.276(8)$ Å) are somewhat shorter than the axial copper–chlorine separations ($\text{Cu}(1)\text{--Cl}(3) = 2.501(8)$ Å, $\text{Cu}(1)\text{--Cl}(2) = 2.533(8)$ Å) and are comparable with those observed in related diazine complexes.²⁷ $\text{Cu}(1)$ and $\text{Cu}(2)$ are displaced by 0.28(1) and 0.37(1) Å, respectively, from the mean planes of the basal donor sets $\text{N}(1)$, $\text{N}(2)$, $\text{Cl}(1)$, $\text{Cl}(3)$ and $\text{N}(3)$, $\text{N}(4)$, $\text{Cl}(2)$, $\text{Cl}(4)$ toward axial chlorine atoms $\text{Cl}(2)$ and $\text{Cl}(1)$, respectively. The molecule is twisted, with the ligand adopting an “anti” conformation and with a dihedral angle of 57.5° between the least-squares planes defining the basal donor sets. Copper–chlorine (terminal) distances (2.245(8), 2.236(7) Å) are normal, but the copper–copper separation (3.224(4) Å) is significantly larger than that observed in $[\text{Cu}_2(\text{BPMTD})(\mu_2\text{-N}_3)(\mu_2\text{-X})\text{X}_2]\cdot\text{CH}_3\text{CN}$ ($\text{X} = \text{Cl}, \text{Br}$) (3.1215–3.138 Å)^{7,19} and other related triply bridged dinuclear copper(II) complexes, e.g. $[\text{Cu}_2(\text{PTPH})\text{Cl}_4]\cdot 2\text{CH}_3\text{OH}$ (3.1194(2) Å) (PTPH = 1,4-bis(2-pyridylthio)phthalazine)² and $[\text{Cu}_2(\text{PTP})\text{Cl}_4]\cdot\text{CH}_3\text{CH}_2\text{OH}$ (3.198(1) Å) (PTP = 3,6-bis(2-pyridylthio)pyridazine),²⁷ which involve a six-membered chelate ring and a six-membered diazine ring. However the azide bridged BPMTD complexes have a “syn” ligand conformation, with the two copper square pyramids bridged equatorially by the azide and axially by the halogen,^{7,19} while in the case of the PTPH complex, despite the “anti” ligand conformation, the combination of the smaller chelate rings and larger diazine ring leads to a smaller dinuclear center. The copper–nitrogen (diazole) distances ($\text{Cu}(1)\text{--N}(2) = 2.21(2)$ Å, $\text{Cu}(2)\text{--N}(3) = 2.27(2)$ Å) are comparable to those observed for the BPMTD azide complexes^{7,19} but are quite long when compared with similar bonds in 3. This may be attributed to the presence of seven-membered chelate rings, which have the effect of pulling the metals away from the diazole bridge.

The structure of 3 is shown in Figure 3, and bond lengths and angles relevant to the copper coordination spheres are given in Table 4. Compound 3 has a structure very similar to that of 1, involving an asymmetric, triple-bridge arrangement (diazole and two halogen bridges). The ligand has an “anti” conformation with a 2-fold rotational axis passing through the sulfur atom and bisecting the N–N bond of the thiadiazole ring. Each copper center has a distorted square-pyramidal structure, bound to the nitrogen atoms of the thiadiazole and pyridine rings, a terminal bromine atom and a bridging bromine atom in the equatorial

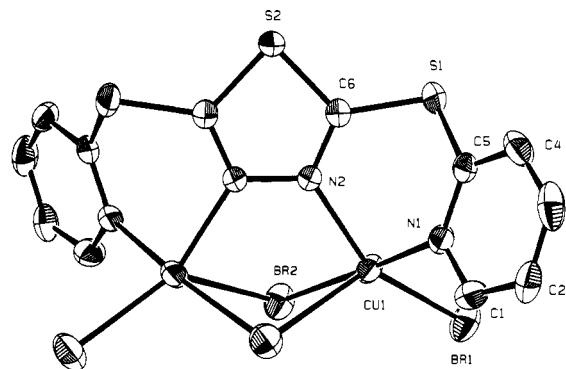


Figure 3. representation of $[\text{Cu}_2(\text{BPTD})\text{Br}_4]$ (3), with hydrogen atoms omitted (40% probability thermal ellipsoids).

Table 4. Intramolecular Distances (Å) and Angles (deg) relevant to the Copper Coordination Spheres in $[\text{Cu}_2(\text{BPTD})(\mu_2\text{-Br})_2\text{Br}_2]$ (3)

$\text{Br}(1)\text{--Cu}(1)$	2.376(1)	$\text{Br}(2)\text{--Cu}(1)$	2.412(1)
$\text{Cu}(1)\text{--N}(1)$	2.034(5)	$\text{Cu}(1)\text{--N}(2)$	2.043(4)
$\text{Cu}(1)\text{--Cu}(1)$	3.556(2)	$\text{Br}(2)\text{--Cu}(1)$	2.861(1)
$\text{Br}(1)\text{--Cu}(1)\text{--Br}(2)$	94.88(4)	$\text{Br}(1)\text{--Cu}(1)\text{--N}(1)$	90.8(1)
$\text{Br}(1)\text{--Cu}(1)\text{--N}(2)$	150.5(1)	$\text{Br}(2)\text{--Cu}(1)\text{--N}(1)$	173.6(2)
$\text{Br}(2)\text{--Cu}(1)\text{--N}(2)$	90.3(1)	$\text{N}(1)\text{--Cu}(1)\text{--N}(2)$	86.1(2)
$\text{Cu}(1)\text{--Br}(2)\text{--Cu}(1)$	84.34(4)		

plane, and an axial bridging bromine atom. The two copper centers are bridged simultaneously by the thiadiazole nitrogen atoms ($\text{N}(2)$, $\text{N}(2)^*$) and two bromine atoms ($\text{Br}(2)$, $\text{Br}(2)^*$) in the familiar axial–equatorial triple-bridge arrangement. The $\text{Cu}(1)\text{--Br}(2)\text{--Cu}(1)^*$ bridge angle of 84.34(4)°, the equatorial copper–bromine distances ($\text{Cu}(1)\text{--Br}(2) = 2.412(1)$ Å, $\text{Cu}(2)\text{--Br}(1) = 2.376(1)$ Å), and the long axial copper–bromine separation ($\text{Cu}(1)\text{--Br}(2)^* = 2.861(1)$ Å) are comparable to those reported for a similar dicopper(II) complex $[\text{Cu}_2(\text{PTP})(\mu_2\text{-Br})_2\text{Br}_2]$ (PTP = 3,6-bis(2-pyridylthio)pyridazine) involving a related tetradentate (N_4) diazine ligand.⁸ The copper centers are displaced by 0.241(3) Å from the mean planes of the basal N_2Br_2 donor sets toward the apical bromine atoms, and the two $\text{N}_2\text{--CuBr}_2$ mean planes are mutually inclined by 25.87°, with a dihedral angle between pyridine mean planes of 80.05°. The Cu–Cu separation of 3.556(2) Å is very large compared with that of 1, as well as with other similar triply bridged dinuclear copper(II) complexes, e.g. $[\text{Cu}_2(\text{PTP})(\mu_2\text{-Br})_2\text{Br}_2]$ (3.318(3) Å),⁸ and is clearly associated with the change from a six-membered pyridazine ring to a five-membered thiadiazole ring. The copper–nitrogen (diazole) distance ($\text{Cu}(1)\text{--N}(2) = 2.043(4)$ Å) is significantly shorter than those observed for 1 and other azido complexes of the ligand BPMTD (2.21–2.27 Å),^{7,19} which is again associated with the difference in the chelate ring size and diazine ring size.

The overall structure of 5 is quite complex and involves the superposition of two intertwined, “zigzag”, polymeric strands, each at 50% occupancy. The structure of a fragment of one strand of 5 is illustrated in Figure 4, and bond distances and angles relevant to the copper coordination spheres are listed in Table 5. Within each strand, the two copper(II) centers are bound to one bridging ligand via the pyridine groups, with the copper atoms being linked by pairs of ligands in a trans arrangement, with two trans-chlorine ligands occupying the other two equatorial coordination sites. In-plane copper–ligand bond distances ($\text{Cu}(1)\text{--Cl}(1) = 2.284(3)$ Å, $\text{Cu}(1)\text{--N}(1) = 2.038(7)$ Å) are fairly short and typical for ligands of this sort. Since the pendant pyridine rings are bonded to the thiadiazole ring via an intervening S–CH₂– group, this creates the potential for exocyclic sulfur interaction with the copper atoms. Copper–sulfur distances ($\text{Cu}(1)\text{--S}(1) = 2.796(6)$ Å, $\text{Cu}(1)\text{--S}(3) = 2.794(6)$ Å), although quite long, are short enough to be considered as ligands to copper, and so the coordination geometry around copper is best described

(27) Mandal, S. K.; Thompson, L. K.; Newlands, M. J.; Lee, F. L.; Le Page, Y.; Charland, J.-P.; Gabe, E. J. *Inorg. Chim. Acta* 1986, 122, 199.

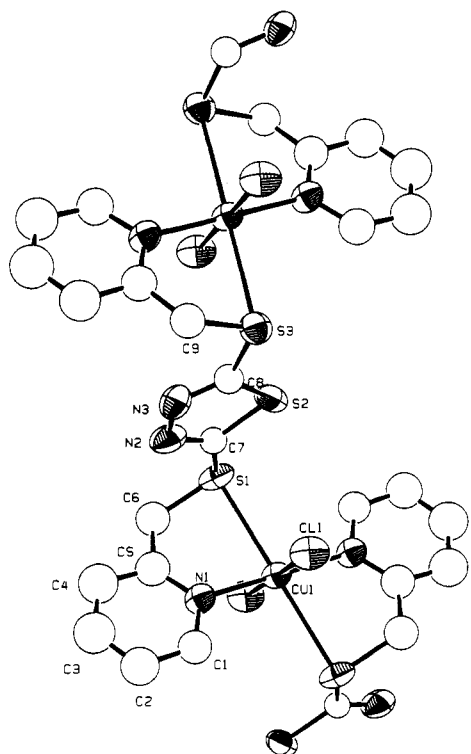


Figure 4. representation of a fragment of one strand of $[\text{Cu}(\text{BPMTD})\text{-Cl}_2]_n$ (**5**), with hydrogen atoms omitted (40% probability thermal ellipsoids).

Table 5. Intramolecular Distances (Å) and Angles (deg) Relevant to the Copper Coordination Sphere in $[\text{Cu}(\text{BPMTD})\text{Cl}]_n$ (**5**)

Cu(1)–Cl(1)	2.284(3)	Cu(1)–Cl(1)′	2.284(3)
Cu(1)–N(1)	2.038(7)	Cu(1)–N(1)′	2.038(7)
Cu(1)–S(1)	2.796(6)	Cu(1)–S(3)	2.794(6)
Cu(1)–Cu(1)′	8.986(4)		
Cl(1)–Cu(1)–Cl(1)′	180.00	Cl(1)′–Cu(1)–N(1)	90.2(2)
Cl(1)–Cu(1)–N(1)	89.8(2)	Cl(1)–Cu(1)–N(1)′	90.2(2)
N(1)–Cu(1)–N(1)′	180.00	Cl(1)′–Cu(1)–N(1)′	89.8(2)
S(1)–Cu(1)–N(1)	79.4(3)	S(3)–Cu(1)–N(1)	81.0(3)
S(1)–Cu(1)–N(1)′	100.6(3)	S(3)–Cu(1)–N(1)′	99.0(3)
S(1)–Cu(1)–Cl(1)	86.2(2)	S(3)–Cu(1)–Cl(1)	97.1(1)
S(1)–Cu(1)–Cl(1)′	93.8(2)	S(3)–Cu(1)–Cl(1)′	82.9(1)
C(6)–S(1)–C(7)	102.1(9)	C(9)–S(3)–C(8)	100(1)
C(6)–S(1)–Cu(1)	87.1(7)	C(9)–S(3)–Cu(1)	87.7(7)
C(7)–S(1)–Cu(1)	108.6(7)	C(8)–S(3)–Cu(1)	105.6(7)

as a distorted octahedron. The angles around the exocyclic sulfur atoms are sufficiently close to the tetrahedral angle to support sulfur bonding, but the copper–sulfur bonds are not exactly at right angles to the CuN_2Cl_2 plane, with angles in the range 79.4–100.6°. This may be attributed to the strained five-membered chelate ring generated by the exocyclic sulfur and pyridine nitrogen atoms. The thiazole rings are not involved in bonding and simply act as rigid spacers linking the copper octahedra.

Spectroscopic Properties. The solid-state, mull transmittance electronic spectrum for compound **1** exhibits multiple absorption bands in the range 600–900 nm (Table 6), which are assigned to d–d transitions in distorted square-pyramidal copper centers, in agreement with the X-ray structure determination. In DMF solution, significant changes in the spectrum suggest a structural change, probably resulting from the replacement of the anions by solvent molecules. This is confirmed by conductance measurements in DMF solution for **1**, which indicate the presence of a 3:1 electrolyte. The solid-state spectra of **2** and **3** exhibit mainly one very broad d–d absorption at around 700 nm (low-energy shoulder for **3**), suggesting the presence of five-coordinate copper centers, in agreement with the X-ray structure determination of

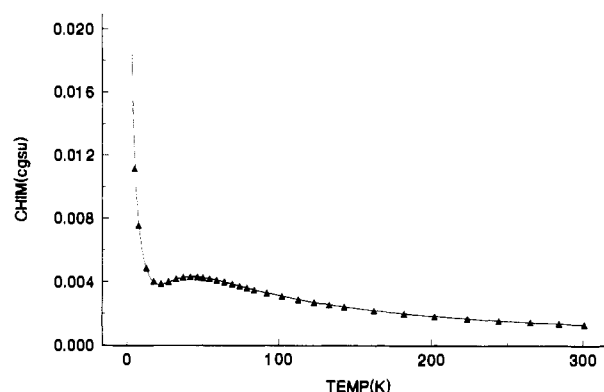


Figure 5. data for $[\text{Cu}_2(\text{BPMTD})\text{Cl}_4]$ (**1**). The solid line was calculated from eq 1, with $g = 2.075(7)$, $-2J = 59.3(7) \text{ cm}^{-1}$, $\rho = 0.148$, and $\theta = -4 \text{ K}$.

3. The general similarities of the infrared and electronic spectra (solid state) for **2** and **3** suggest that **2** has a similar structure in the solid state. In DMF solution, **2** and **3** each exhibit a large shift in the position of their d–d absorption bands to lower energy (Table 6), suggesting a change in the coordination environment at the copper centers by solvent ligation. Conductance measurements carried out in DMF ($\Lambda_m(25 \text{ }^\circ\text{C}) = 159$ (**2**), 218 (**3**) $\text{mhos mol}^{-1} \text{ cm}^2$) indicate the formation of 2:1 and 3:1 electrolytes, respectively. An infrared absorption band at 3512 cm^{-1} for **4** is assigned to $\nu(\text{OH})$ of a bridging hydroxy group. The presence of three nitrate combination ($\nu_1 + \nu_4$) absorptions at 1754, 1724, and 1720 (shoulder) cm^{-1} suggests the presence of different nitrate groups.²⁸ Since the Cu–Cu separation is likely to be in excess of 3.5 Å (cf. 3.556(2) Å for **3**), it would seem unlikely that a nitrate could act as an axial bidentate bridge in **4**, a bonding mode found in dinuclear copper(II) complexes with six-membered diazine (phthalazine) rings, six-membered chelate rings, and much shorter Cu–Cu separations (approximately 3.1 Å).¹ The most reasonable interpretation of these data suggests the presence of a bidentate nitrate at each copper center and an ionic nitrate. These spectral data for **4** are consistent with a dinuclear structure with equatorial hydroxide and diazole groups bridging two square-pyramidal copper centers, with a bidentate nitrate at each copper center, linking axial and equatorial sites. A single d–d absorption at 610 nm supports the presence of five-coordinate copper centers with CuN_2O_3 chromophores. High-intensity absorptions are observed in most cases in the region 310–420 nm, associated with charge-transfer transitions.

The solid-state, mull transmittance electronic spectrum of **5** exhibits three prominent d–d bands in the range 600–900 nm, which can reasonably be associated with a highly distorted six-coordinate $\text{CuN}_2\text{S}_2\text{Cl}_2$ species. The powder ESR spectrum of **5** exhibits three distinct g values ($g_1 = 2.064$, $g_2 = 2.092$, $g_3 = 2.185$ at room temperature), typical of an elongated rhombic species, both at room temperature and 77 K.

Magnetic Properties. Room-temperature magnetic moments for compounds **1–4** fall in the range 1.03–1.68 μ_B/Cu (Table 6), which are lower than the value expected for a one-unpaired-electron species and are indicative of the presence of antiferromagnetic exchange interactions between the adjacent copper(II) centers. Compound **5** has a normal magnetic moment and is not expected to exhibit any spin-exchange interactions. Variable-temperature magnetic studies were carried out on powdered samples of **1–4** in the temperature range 4–300 K. Magnetic susceptibility data are plotted as a function of temperature for **1** (X-ray sample) in Figure 5. The profile is characterized by a maximum at about 45 K, with a rapid rise in susceptibility at lower temperatures. This plot is indicative of a weakly antiferromagnetically coupled system with a large proportion of dilute,

(28) Lever, A. B. P.; Mantovani, E.; Ramaswamy, B. S. *Can. J. Chem.* **1971**, *49*, 1957.

Table 6. Magnetic, Spectral, and Electrochemical Data

complex	μ_{eff} at room temp (μ_B)	electronic data (nm) ($\epsilon = \text{L mol}^{-1} \text{cm}^{-1}$)	electrochemistry ^c $E_{1/2}$ (V vs SCE) (ΔE_p (mV)) (100 mV s ⁻¹)
[Cu ₂ (BPMTD)(μ_2 -Cl) ₂ Cl ₂] 2CH ₃ OH·0.5CH ₃ CN (1)	1.61	900, 750, 610, 360 ^a 925 (175), [830] (160), 435 (470) ^b	0.43 (120)
[Cu ₂ (BPTD)(μ_2 -Cl) ₂ Cl ₂] (2)	1.68	710, 405, ^a 925 (350), 440 (1160), 310 (22 500) ^b	0.435 (130)
[Cu ₂ (BPTD)(μ_2 -Br) ₂ Br ₂] (3)	1.59	[830], 700, 420, ^a 930 (290), 580 (325), [485] (425), 310 (32 600) ^b	0.48 (120)
[Cu ₂ (BPTD)(μ_2 -OH)(NO ₃) ₃] (4)	1.03	610 ^a	
[Cu(BPMTD)Cl ₂] _n (5)	1.77	860, 725, 600 ^a	

^a Mull transmittance. ^b DMF ([] = shoulder). ^c GC/DMF/TEAP/SCE.

Table 7. Magnetic Data

complex	g	$-2J$ (cm ⁻¹)	TIP (10 ⁶ cgsu)	ρ	10 ² R ^a	Θ , K
[Cu ₂ (BPMTD)(μ_2 -Cl) ₂ Cl ₂] 2CH ₃ OH·0.5CH ₃ CN (1)	2.075(7)	59.3(7)	58	0.148	0.53	-4
[Cu ₂ (BPTD)(μ_2 -Cl) ₂ Cl ₂] (2)	2.039(5)	34.9(3)	50	0.053	0.22	0.4
[Cu ₂ (BPTD)(μ_2 -Br) ₂ Br ₂] (3)	2.032(7)	69.4(9)	90	0.036	2.4	-3
[Cu ₂ (BPTD)(μ_2 -OH)(NO ₃) ₃] (4)	2.18(2)	529(5)	70	0.016	0.66	0.2

^a $R = [\sum(\chi_{\text{obs}} - \chi_{\text{calc}})^2 / \sum(\chi_{\text{obs}})^2]^{1/2}$.

paramagnetic impurity. The variable-temperature susceptibility data were fitted to the Bleaney-Bowers expression (eq 1)²⁹ for

$$\chi_m = \frac{N\beta^2 g^2}{3k(T - \Theta)} \left[1 + \frac{1}{3} \exp(-2J/kT) \right]^{-1} (1 - \rho) + \frac{(N\beta^2 g^2)\rho}{4kT} + N\alpha \quad (1)$$

exchange-coupled pairs of copper(II) ions. In this expression $2J$ (in the spin Hamiltonian $H = -2J\hat{s}_1 \cdot \hat{s}_2$) is the singlet-triplet splitting or the exchange integral and other symbols have their usual meaning. χ_m is expressed per mole of copper atoms, $N\alpha$ is the temperature-independent paramagnetism (TIP), Θ is a corrective term for intermolecular associations,^{30,31} and ρ represents the fraction of a magnetically dilute impurity. The parameters giving the best fit were obtained using a nonlinear regression analysis with g , J , ρ , and Θ as variables, and the results are presented in Table 7. The results of the best fit are shown as the solid line in Figure 5 for $g = 2.075(7)$, $-2J = 59.3(7) \text{ cm}^{-1}$, $\rho = 0.148$, and $\Theta = -4 \text{ K}$. The data fit could only be obtained using a large proportion of paramagnetic impurity. This probably indicates that, even in its complexed form, the ligand BPMTD is unstable and that an internal redox reaction is taking place in the solid state, with the formation of a mononuclear copper(II) or mixed-valence (Cu^{II}/Cu^I) paramagnetic species. The crystalline sample used in the X-ray analysis developed cracks on standing, and a number of peaks in the difference map were not identified. A solid-state ESR spectrum of the same sample of 1 showed a strong, largely isotropic signal at $g_{\text{av}} = 2.10$, suggesting the presence of isolated copper(II) centers. The small Θ correction suggests the presence of weak intermolecular antiferromagnetic exchange, but in view of the large ρ correction, the significance of this term should perhaps be downplayed.

Variable temperature magnetic data for 2 are illustrated in Figure 6. A maximum in the profile around 30 K indicates weak antiferromagnetic coupling between the copper centers, and a nonlinear regression analysis of the data using eq 1 gave $g = 2.039(5)$, $-2J = 34.9(3) \text{ cm}^{-1}$, $\rho = 0.053$, and $\Theta = 0.4 \text{ K}$. The solid line in Figure 6 is based on these parameters. Once again, a small, but significant, amount of paramagnetic impurity is necessary for a good fit of the data and suggests that even for the BPTD complexes, where the presence of six-membered chelate

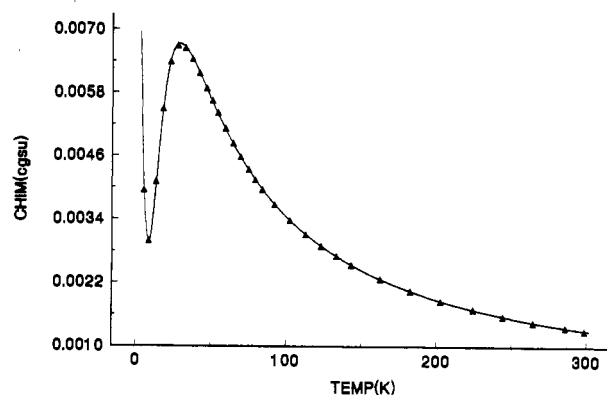


Figure 6. data for [Cu₂(BPTD)Cl₄] (2). The solid line was calculated from eq 1, with $g = 2.039(5)$, $-2J = 34.9(3) \text{ cm}^{-1}$, $\rho = 0.053$, and $\Theta = 0.4 \text{ K}$.

rings would be expected to produce a more stable complex, some decomposition is occurring, probably via hydrolytic cleavage of the ligand and the formation of a mononuclear copper(II) or mixed-valence-state species. Despite a less than ideal data fit for compound 3 (Table 7), it is clear that antiferromagnetic coupling in the bromo complex of BPTD is much larger. Although structural details for 2 are not available, a similar structure is anticipated, on the basis of other spectral similarities, involving an equatorially bound diazine group and orthogonal bridging chlorine atoms. The difference in exchange between 2 and 3 is consistent with previous observations on isostructural pairs of chloro and bromo complexes, where, due to an apparent polarization effect on the part of the terminal and bridging halogens, copper unpaired spin is localized at the copper centers more in the complexes involving the more electronegative chlorine ligands, leading to reduced antiferromagnetic coupling.^{8,32,33}

Variable-temperature magnetic data for 4 (Figure 7) indicate the presence of strong antiferromagnetic coupling ($-2J = 529(5) \text{ cm}^{-1}$) (Table 7) between the two copper(II) centers, thus confirming the presence of an equatorial hydroxide bridge, which provides an effective superexchange pathway for spin coupling between the $d_{x^2-y^2}$ magnetic orbitals on the adjacent copper centers. The small exchange integrals for 1-3 indicate that the hydroxide bridge in 4 is responsible for most of the spin coupling in this compound.

The axial/equatorial triple-bridge arrangement in 1 and 3, and supposedly in 2, creates a superexchange situation where the

(29) Bleaney, B.; Bowers, K. D. *Proc. R. Soc. London* 1952, A214, 451.

(30) McGregor, K. T.; Barnes, J. A.; Hatfield, W. E. *J. Am. Chem. Soc.* 1973, 95, 7993.

(31) Sikorav, S.; Bkouche-Waksman, I.; Kahn, O. *Inorg. Chem.* 1984, 23, 490.

(32) Thompson, L. K.; Mandal, S. K.; Gabe, E. J.; Lee, F. L.; Addison, A. W. *Inorg. Chem.* 1987, 26, 657.

(33) Mandal, S. K.; Thompson, L. K.; Newlands, M. J.; Gabe, E. J. *Inorg. Chem.* 1990, 29, 1324.

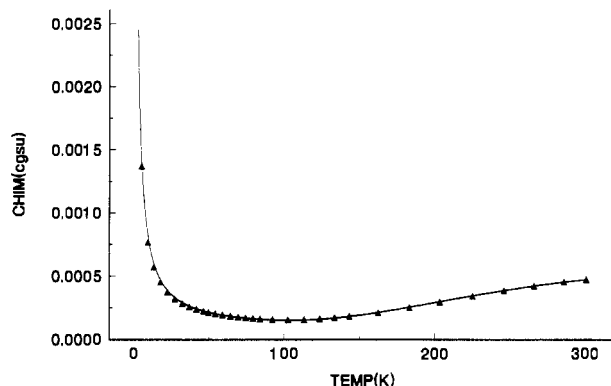


Figure 7. data for $[\text{Cu}_2(\text{BPTD})(\text{OH})(\text{NO}_3)_3]$ (4). The solid line was calculated from eq 1, with $g = 2.18(2)$, $-2J = 529(5) \text{ cm}^{-1}$, and $\theta = 0.2 \text{ K}$.

orthogonal halogen bridges do not contribute in an antiferromagnetic sense, even though they may moderate exchange, and so the diazine bridge is regarded as the only viable pathway for antiferromagnetic superexchange. However the thiadiazole bridge appears to be an example of a weak diazine superexchange bridge. This is in contrast to the situation for 1:1 dinuclear copper(II) complexes of bpt ($\text{bptH} = 3,5\text{-bis}(\text{pyridin-2-yl})\text{-1,2,4-triazole}$; $-J = 102\text{--}118 \text{ cm}^{-1}$)³⁴ and aamt ($\text{aamt} = 4\text{-amino-3,5-bis}(\text{aminomethyl})\text{-1,2,4-triazole}$; $-J = 99\text{--}112 \text{ cm}^{-1}$)³⁵ involving an almost planar arrangement of two triazole diazine bridges linking the two copper centers.

In the absence of any significant ferromagnetic contribution from the halogen bridges themselves, a comparison of the related complexes $[\text{Cu}_2(\text{PTP})\text{X}_4]$ ($\text{X} = \text{Cl}, \text{Br}$)^{8,27} $[\text{Cu}_2(\text{PTPH})\text{X}_4]$ ($\text{X} = \text{Cl}, \text{Br}$)² and 2 and 3, all of which have six-membered chelate rings, orthogonal dihalogen bridges, and comparable Cu–N (diazine) and N–N (diazine) distances (no structural data for 2), indicates the superexchange order pyridazine > phthalazine > thiadiazole. The improved exchange efficiency of pyridazine over phthalazine has also been demonstrated in other systems involving just diazine bridges between $d_{x^2-y^2}$ ground-state copper(II) centers⁵ and is related to the capacitive action of the fused benzene ring in phthalazines. Both phthalazine and pyridazine groups have extensive π delocalization within the aromatic rings, a feature which would be expected to be weaker in the thiadiazole bridge.

The question of whether the spin-exchange process involves σ or π mechanisms or both in heterocyclic 1,2-diazine-bridged systems is an intriguing one and can perhaps be addressed to some extent by comparing this sort of dinuclear species with the complex $\text{Cu}_2(\text{PMK})\text{Cl}_4$ ($\text{PMK} = \text{bis}(2\text{-pyridylmethyl})\text{ketazine}$).³⁶ This complex has a twisted trans structure in which the copper(II) centers are bridged just by the N–N fragment and the ligand is nonplanar. Such a bridge arrangement would, of necessity, have limited π involvement, and so the superexchange pathway would be largely σ in nature. For this compound $-2J = 52(4) \text{ cm}^{-1}$, which is comparable with the values obtained for the thiadiazole complexes. A related diazine–dioxime complex, $\text{Cu}_2(\text{H}_2\text{doxN}_2)\text{Cl}_4$ ³⁷ ($-2J = 38.5(2) \text{ cm}^{-1}$), again involving a twisted diazine bridging fragment, strengthens this argument of σ superexchange. This being the case, the extent of π spin transfer in 1–3 may be very small. The ring sulfur atom would not be expected to exert a significant spin polarization effect, due to its low electronegativity, and so the principal portion of the thiadiazole

ring responsible for antiferromagnetic exchange would be the N–N group.

These results therefore suggest that a significant portion of the exchange capacity of aromatic π -ring 1,2-diazines like triazole, pyridazine, and phthalazine involves a π -transfer mechanism. Broad-line NMR studies on pyridazine-, phthalazine-, and triazole-bridged polymeric copper(II) complexes³⁸ show that negative spin densities reside on the ring carbon atoms adjacent to the diazine nitrogens. This occurs as a result of π -bond conjugation with the nitrogen atoms, which assume a positive spin density as a result of copper–nitrogen σ -bond formation. An extended π system like phthalazine has four carbons with negative spin densities, as a result of extended π conjugation (as opposed to two for pyridazine), and so can accumulate more negative charge delocalized from the copper atoms, in agreement with the earlier experimental observations indicating $-2J_{\text{pyridazine}} > -2J_{\text{phthalazine-2,5,8,27,39}}$.

Electrochemistry. The electrochemical properties of the dinuclear copper(II) complexes 1–3 were studied by cyclic voltammetry in the range -1.0 to $+0.6 \text{ V}$ in DMF solution containing 0.1 M tetraethylammonium perchlorate (TEAP) as supporting electrolyte at a glassy carbon electrode. Cyclic voltammograms for these dinuclear complexes are very similar and involve just one quasi-reversible redox wave at positive potentials ($E_{1/2} = 0.43\text{--}0.48 \text{ V}$ vs SCE) (Table 6). Conductance data indicate that these solution species are solvated, with several coordinated halogens displaced by DMF. Coulometric studies on green solutions of 2 and 3 ($E = 0.1 \text{ V}$ (2), $E = -0.1 \text{ V}$ (3); potentials corrected appropriately for the Ag wire reference electrode) indicate passage of slightly less than 2 electron equiv of charge on reduction (1.7 for 2, 1.8 for 3), with the formation of colorless solutions. Reoxidation of the solution of 2 at $+0.70 \text{ V}$ required exactly 2 electron equiv of charge. Reoxidation of 3 at the same potential was complicated by the oxidation of bromide also, and so an accurate coulomb count could not be obtained. These data confirm that the redox processes are associated with reduction of the copper(II) centers to copper(I).

The fact that less than two electrons/mol were required to reduce 2 and 3 to copper(I) species is consistent with the magnetic data for these compounds, which indicate the presence of significant paramagnetic impurities. Also, the fact that clean, single waves are observed in the wide potential range chosen suggests that the partially reduced species are probably dinuclear Cu(II)/Cu(I) complexes involving some copper(II) sites which have been reduced to copper(I). The general electrochemical properties of these complexes compare closely with those of other related dinuclear copper(II) systems involving tetradentate (N_4) diazine ligands, all of which exhibit Cu(II)/Cu(I) redox processes at positive potentials.^{32,40,41}

Conclusion

Two new tetradentate, dinucleating thiadiazole ligands (BPMTD, BPTD) have been isolated and their dinuclear copper(II) complexes synthesized and characterized structurally through spectroscopic, magnetic, and X-ray diffraction studies. Tetrahalide derivatives (1–3), which involve a triple-bridge arrangement (diazole and two asymmetric halogen bridges) between the copper(II) centers, are weakly antiferromagnetically coupled ($-2J = 34\text{--}60 \text{ cm}^{-1}$), where the main superexchange pathway responsible for antiferromagnetic coupling is the diazole diazine bridge. Compound 4, which exhibits strong antiferromagnetic coupling ($-2J = 529 \text{ cm}^{-1}$) between the two adjacent copper centers, appears

(34) Prins, R.; Birker, P. J. M. W. L.; Haasnoot, J.; Verschoor, G. C.; Reedijk, J. *Inorg. Chem.* 1985, 24, 4128.

(35) Koomen-van Oudenniel, W. M. E.; de Graff, R. A. G.; Haasnoot, J. G.; Prins, R.; Reedijk, J. *Inorg. Chem.* 1989, 28, 1128.

(36) O'Connor, C. J.; Romananch, R. J.; Robertson, D. M.; Eduok, E. E.; Fronczek, F. R. *Inorg. Chem.* 1983, 22, 449.

(37) Batiz, R.; Brémard, C.; Nowogrocki, G.; Sœur, S. *Polyhedron* 1990, 9, 2663.

(38) Emori, S.; Inoue, M.; Kubo, M. *Bull. Chem. Soc. Jpn.* 1972, 45, 2259.

(39) Abraham, F.; Lagrenee, M.; Sœur, S.; Mernari, B.; Brémard, C. *J. Chem. Soc., Dalton Trans.* 1991, 1443.

(40) Thompson, L. K.; Mandal, S. K.; Rosenberg, L.; Lee, F. L.; Gabe, E. *J. Inorg. Chim. Acta* 1987, 133, 81.

(41) Mandal, S. K.; Thompson, L. K.; Gabe, E. J.; Lee, F. L.; Charland, J.-P. *Inorg. Chem.* 1987, 26, 2384.

to involve two equatorial bridges (diazole and hydroxo bridges) in a symmetric bridged arrangement, which is responsible for more effective overlap with the copper $d_{x^2-y^2}$ magnetic orbitals, thus providing more efficient superexchange pathways, but clearly is dominated by the hydroxide bridge.

BPMTD produces rather unstable dinuclear copper(II) halide complexes containing significant amounts of dilute copper(II) impurities, attributable to ligand decomposition. However, BPMTD appears to be quite stable in a polymeric, 1-dimensional

(NS) chain complex (II), in which the thiadiazole group does not coordinate to the copper(II) centers.

Acknowledgment. We thank the Natural Sciences and Engineering Research Council of Canada for financial support for this study and for funds to purchase the X-ray diffractometer.

Supplementary Material Available: Tables listing detailed crystallographic data, hydrogen atom positional parameters, anisotropic thermal parameters, bond lengths and angles, and least-squares planes (17 pages). Ordering information is given on any current masthead page.